

RESEARCH ARTICLE

Whither warming in the Galápagos?

Kristopher B. Karnauskas ^{1,2*}

1 Department of Atmospheric and Oceanic Sciences, University of Colorado Boulder, Boulder, CO, United States of America, **2** Cooperative Institute for Research in Environmental Sciences, University of Colorado Boulder, Boulder, CO, United States of America

* kristopher.karnauskas@colorado.edu

Abstract

The Galápagos Islands play host to an iconic ecosystem—a UNESCO World Heritage Site and the second largest marine reserve in the world, home to several endangered species. The waters off the west coast of the Galápagos are also one of the few places in the world ocean that are presently cooling, with potentially significant ecological consequences of this local reprieve from global warming. Here I show, using a recently developed high-resolution ocean state estimate, that the observed cooling in the Galápagos is the result of a strengthening of the wind-driven equatorial ocean circulation. An acceleration and shift of the Equatorial Undercurrent, which can be attributed to a strengthening of the cross-equatorial component of the trade wind in response to the interhemispheric gradient in surface warming, leads to a 54% increase in upwelling velocity along the western Galápagos Islands as well as increased shear-induced mixing. Analogous to other so-called “cold blobs,” such as the one south of Greenland in the North Atlantic, this is an early and important sentinel of a broader change in the tropical ocean circulation. Thus far, and for perhaps the very near future, the western shores of the Galápagos appear to offer refuge from some of the deleterious impacts of anthropogenic climate change including suppressed upwelling and surface warming.

 OPEN ACCESS

Citation: Karnauskas KB (2022) Whither warming in the Galápagos? PLOS Clim 1(9): e0000056. <https://doi.org/10.1371/journal.pclm.0000056>

Editor: Andrea Storto, National Research Council, ITALY

Received: January 24, 2022

Accepted: July 28, 2022

Published: September 7, 2022

Copyright: © 2022 Kristopher B. Karnauskas. This is an open access article distributed under the terms of the [Creative Commons Attribution License](https://creativecommons.org/licenses/by/4.0/), which permits unrestricted use, distribution, and reproduction in any medium, provided the original author and source are credited.

Data Availability Statement: All three primary data sets used in this study are freely and publicly available. The NOAA Olv2 SST data set is available for download from NOAA: <https://www.esrl.noaa.gov/psd/data/gridded/data.noaa.oisst.v2.highres.html> GLORYS-12v1 fields are available for download from the Copernicus Marine Service: https://resources.marine.copernicus.eu/?option=com_csw&view=details&product_id=GLOBAL_REANALYSIS_PHY_001_030 ERA5 fields are available for download from the Copernicus Climate Change Service: <https://cds.climate.copernicus.eu/#!/search?text=ERA5&type=dataset> High-resolution coastlines plotted in Figs 1, 2, 3, 4

Introduction

There are only a few places in the world ocean where the surface temperature is not increasing, and rightfully, they tend to be foci of scientific intrigue. The high latitude North Atlantic Ocean is one of them, where an observed cooling trend may be the fingerprint of a slowdown of the Atlantic Meridional Overturning Circulation [1, 2]. The Galápagos is another [3, 4], and despite its iconic marine ecosystem hosting several endangered species including the Galápagos penguin [5], Galápagos fur seal [6] and Galápagos sea lion [7], its status as a “living museum and showcase of evolution” according to the UNESCO World Heritage Convention [8], and its conspicuous placement within the eastern equatorial Pacific Ocean where subtle fluctuations have profound global impacts (*i.e.*, El Niño [9, 10]), the coupled dynamics of this system and its recent changes have received comparatively little attention.

Viewed from space, the Galápagos Archipelago is but a dot in an otherwise enormous ocean basin. However, the very dynamics governing the equatorial oceans also confer upon

and 6 are from the Global Self-consistent, Hierarchical, High-resolution Geography (GSHHG) database version 2.2.3, available for download from NOAA: <https://www.ngdc.noaa.gov/mgg/shorelines/gshhs.html>.

Funding: K.B.K. acknowledges support from the NASA Sea Level Change Science Program, Award 80NSSC20K1123. The funders had no role in study design, data collection and analysis, decision to publish, or preparation of the manuscript.

Competing interests: I have read the journal's policy and the authors of this manuscript have the following competing interests: K.B.K. is a member of the editorial board of PLOS Climate.

the Galápagos a unique oceanographic influence significantly beyond that expected from its physical dimensions alone [11–14]. Because the Galápagos straddles the equator in the eastern Pacific, its oceanographic environs are shaped by the large-scale, wind-driven upwelling spanning most of the equatorial Pacific Ocean, intense local upwelling and mixing due to the upward deflection of the Equatorial Undercurrent (EUC) by the islands themselves [15], and a confluence of surface currents and countercurrents originating in both hemispheres. A recent modeling study has also indicated a key role for submesoscale turbulence and shallow overturning cells, the dynamics of which are critically dependent upon latitude, in maintaining the cool and productive waters west of the Galápagos [16]. As such, and purely by accident of geology, the Galápagos hosts a remarkably well-suited environment for marine animals and seabirds typically associated with higher-latitude climates such as penguins (*Spheniscus mendiculus*), fur seals (*Arctocephalus galapagoensis*), and sea lions (*Zalophus wollebaeki*), all of which are endangered [5–7] and acutely sensitive to seasonal, interannual, and longer-term ocean/climate variability [17–19].

Satellite observations [20] indicate that the cold pool situated adjacent to the Galápagos Archipelago at 92°W in the eastern equatorial Pacific has cooled by about a half a degree centigrade over the past four decades (Fig 1A–1C), quite the opposite of the surrounding region and indeed most of the global ocean (Fig 1D). This steady cooling trend represents a doubling of the intensity of the Galápagos cold pool (GCP), taken relative to sea surface temperatures (SST) throughout the broader eastern equatorial Pacific region (Fig 1E). This trend has potentially significant ecological implications; two thirds of the Galápagos penguin population, for example, lives along a roughly 50-km long stretch of the western coastline of Isabela [21]. Like Kiribati in the central Pacific [22, 23], could the western Galápagos Archipelago be another potential marine refuge from global warming? And like the North Atlantic, is this another

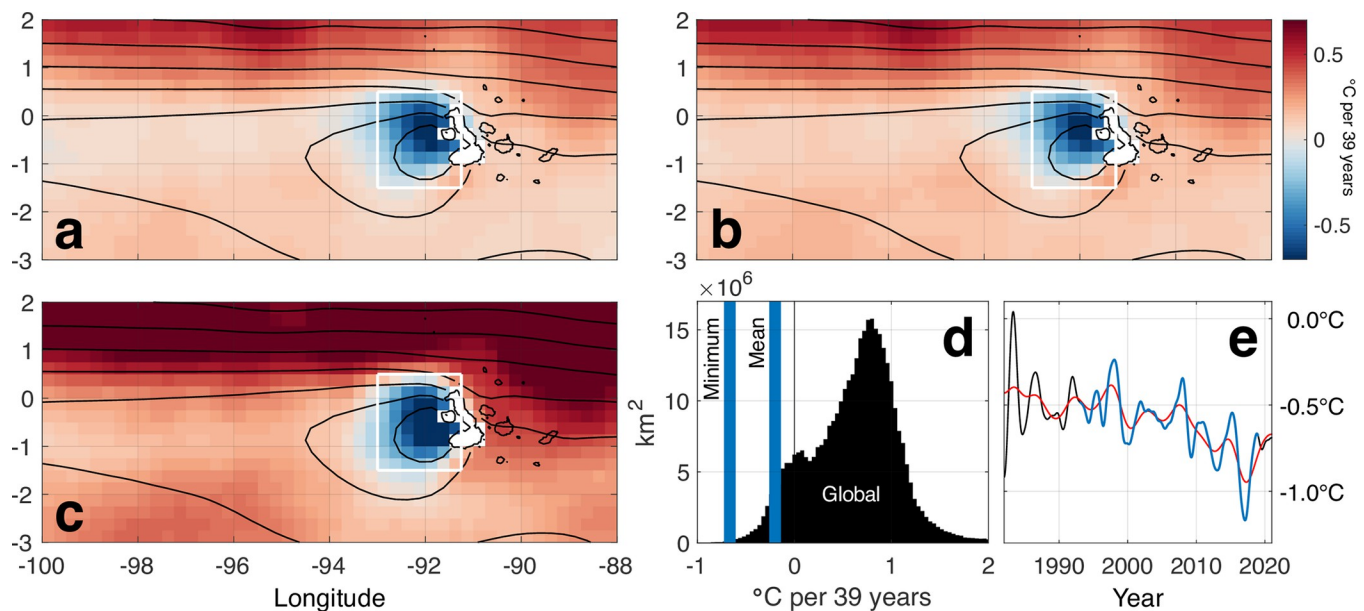


Fig 1. Observed sea surface temperature trends. a, SST trend (°C per 39 years) from Jan. 1982 through Dec. 2020. Black contours are the mean SST, contoured every 0.5°C; the innermost contour is 23°C. b, As in a but with the influence of large ENSO events removed prior to calculating the trend. c, as in a but for the period Jan. 1993 through Dec. 2018. The color scale next to b applies to all three trend maps (a–c). d, Histogram of SST trends throughout the world ocean (one for each square km), with the minimum and mean SST trend in the GCP region (white boxes in a–c) denoted by blue lines. e, Time series of SST averaged within the GCP region relative to the region west of the GCP (extending from the GCP to 100°W) with two (black line) and five (red line) year low-pass filters to remove high-frequency noise. The blue curve outlines the segment of the two year low-pass filtered time series spanning Jan. 1993 through Dec. 2018.

<https://doi.org/10.1371/journal.pclm.0000056.g001>

fingerprint of a changing ocean circulation—albeit subject to different physical mechanisms? Sustained satellite observations, recent advances in data assimilation and the availability of high-resolution oceanic (and atmospheric) state estimates [24, 25] now enable us to answer such questions.

Materials and methods

Sea surface temperature

The National Oceanic and Atmospheric Administration (NOAA) Optimal Interpolation version 2 (OIV2) data are used to evaluate SST trends in the eastern equatorial Pacific from Jan. 1982 through Dec. 2020. The NOAA OIV2 data are provided with daily temporal resolution and 0.25° (~ 25 km) horizontal resolution [20]. The NOAA OIV2 data are a blend of infrared satellite retrievals from the Advanced Very High Resolution Radiometer (AVHRR) and *in situ* measurements from the International Comprehensive Ocean Atmosphere Data Set (ICOADS) [26]. This SST data set is suitable for distinguishing features at the spatial scale of the GCP because the GCP (and the cooling trend observed there) encompasses at least 56 individual 0.25° grid cells (*i.e.*, the white box drawn on Fig 1A–1C).

Linear trends are estimated by least-squares regression. Interannual climate variations in the eastern equatorial Pacific are dominated by the El Niño–Southern Oscillation (ENSO). To ensure that the SST trends are not influenced significantly by the distribution of such events within the 39-year record, an alternate version of the SST trend map is produced wherein data from all days in which the absolute value of the NINO3 index (a typical measure of ENSO, the area averaged SST anomalies between 5°S – 5°N , 150°W – 90°W) exceeded 2 standard deviations were omitted prior to calculation of the trends (Fig 1B). The trend in that case is almost indistinguishable from the trend computed over the full, continuous record. Moreover, an alternative version of the trend map is computed only over 1993–2018 (Fig 1C), the period for which the GLORYS-12v1 ocean reanalysis is available (see below) and for which the subsequent analyses of changes in ocean circulation are calculated. Again, the SST trend map is not qualitatively different from that computed using the full period.

Ocean state and circulation

For estimates of changes in the subsurface ocean thermodynamic state and circulation covering two thirds of the period for which the NOAA OIV2 data are available (1993–2018), the GLObal Ocean ReanalYsis and Simulation (GLORYS)-12v1 product [24] is used. GLORYS-12v1 is a relatively new global ocean, eddy-resolving reanalysis covering the altimeter era at $1/12^\circ$ (~ 9 km) horizontal resolution on 50 vertical levels. The ocean model component is the NEMO platform driven at surface by the ERA5 reanalyses (see below) for recent years. Oceanographic observations are assimilated by means of a reduced-order Kalman filter, and 3D-VAR provides a correction for the slowly-evolving large-scale biases in temperature and salinity. Along track altimetry, SST, sea ice concentration and *in situ* temperature and salinity profiles are jointly assimilated. Daily and monthly means are available—monthly means are used here.

Unlike most current ocean models and ocean state estimates/reanalyses, GLORYS-12v1 includes an exceptionally well resolved Galápagos Archipelago, and a mean zonal circulation at 93°W that validates very well against recent *in situ* observations [27, 28] (Fig 2). These two aspects of the GLORYS-12v1 reanalysis render it uniquely well suited for the present study. Although GLORYS-12v1 is available for only 26 years (1993–2018), all trends are expressed as per 39 years simply to maintain consistency with the observed SST trends that are attempted to be diagnosed, not meant as an explicit assumption that the long-term linear trends must be perfectly invariant from one decade to the next. The similarity between the observed SST

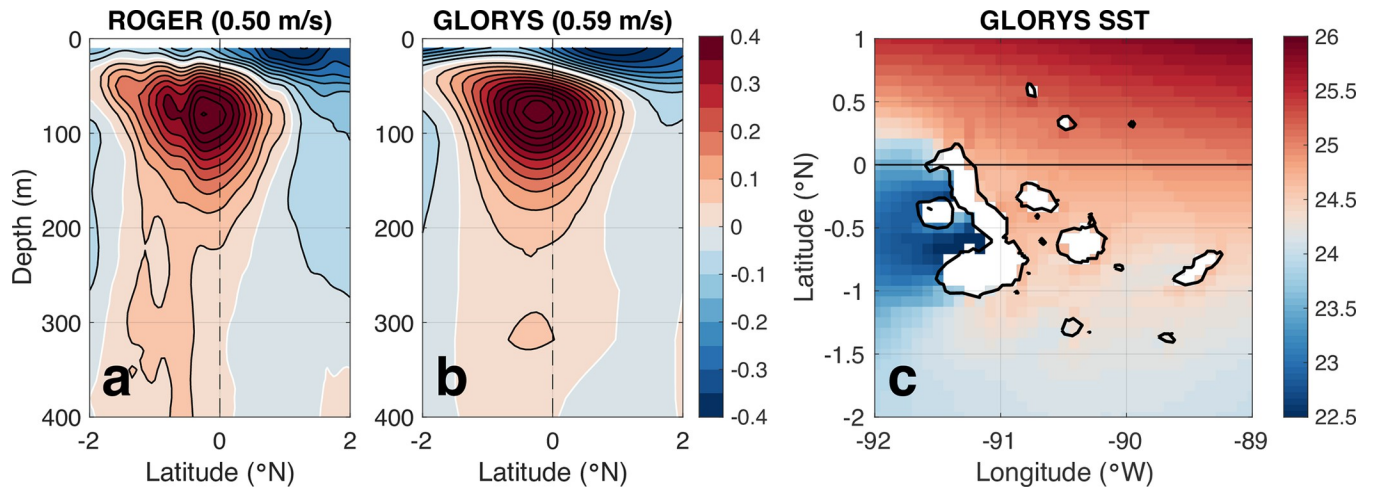


Fig 2. Representation of the EUC and the Galápagos in GLORYS. **a**, Cross-section of mean zonal velocity (m/s) along 93°W from recent glider observations. Contour interval 0.05 m/s with 0 m/s denoted by the white line. The maximum eastward velocity is indicated in the title **b**, As in **a** but from GLORYS. **c**, Map of mean sea surface temperature (°C) in GLORYS with white grid cells indicating the GLORYS land mask representing the Galápagos Islands compared to real coastlines (black contours).

<https://doi.org/10.1371/journal.pclm.0000056.g002>

trend maps for the two periods, 1982–2020 and 1993–2018 (Fig 1), suggests this may be a defensible assumption anyway.

As with all numerical models and reanalyses that are based upon them, results can be dependent on parameterizations of sub-grid scale processes such as mixing. The vertical stratification, shear, and their ratio (a proxy for the tendency for turbulent mixing) are estimated using GLORYS-12v1 data by calculating the buoyancy frequency squared (N^2), shear squared (Sh^2), and the gradient Richardson number (Ri), respectively, as follows:

$$N^2 = -\frac{g}{\rho} \frac{\partial \rho}{\partial z} \tag{1}$$

$$Sh^2 = \left(\frac{\partial u}{\partial z}\right)^2 \tag{2}$$

$$Ri = \frac{N^2}{Sh^2} \tag{3}$$

where g is gravity (9.81 m/s^2), ρ is potential density, and u is zonal ocean velocity. Small values of the gradient Richardson number generally indicate conditions in which the destabilizing effect of shear is sufficient to overcome the stabilizing effect of stratification. The gradient Richardson number results are thus presented as $1/Ri$ to describe the tendency for turbulent mixing to occur. It is important to note that, although Ri and its constituent terms N^2 and Sh^2 are calculated “offline” using basic outputs such as temperature, salinity, and horizontal velocity, which may have reasonable multidecadal tendencies as constrained by assimilated observations, their solutions are not free from the influence of a model’s numerical schemes such as grid scale closures for buoyancy and momentum.

Surface winds

Finally, for estimates of changes in the surface wind field, the ERA5 reanalysis [25] is used. ERA5 is the latest version of the global atmospheric reanalysis from ECMWF, covering the

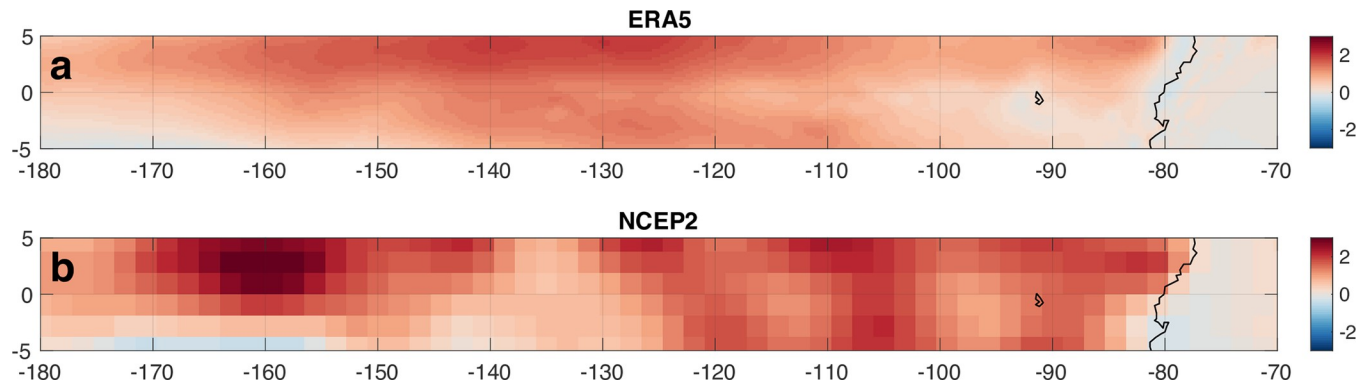


Fig 3. Cross-validation of surface wind trend. **a.** Trend in 10-m meridional wind (m/s per 39 years) in the ERA5 reanalysis from 1982–2020. **b.** As in **a** but for the NCEP2 reanalysis; same time period.

<https://doi.org/10.1371/journal.pclm.0000056.g003>

period 1979 to the present. Monthly mean 10-m wind and sea level pressure fields are provided at 0.25° horizontal resolution. This atmospheric reanalysis is the ideal choice because it was a source of surface forcing to the GLORYS-12v1 ocean reanalysis, thus ensuring physical consistency of the atmospheric and oceanic diagnostic results. However, several other global atmospheric reanalyses are available, albeit not always with such fine horizontal resolution. The most important result derived from ERA5 in this study is the southerly wind trend over the eastern equatorial Pacific from 1982–2020. This result is well reproduced using the NOAA NCEP2 atmospheric reanalysis [29] (Fig 3), thus ensuring this result is robust and not an artifact of how data are assimilated in one reanalysis.

Results

A subtle adjustment at the equator

The Pacific EUC is among the strongest and most coherent ocean currents in the world, with peak volume transport exceeding 40 Sv [30] (1 Sverdrup [Sv] = 1 million cubic meters per second [$10^6 \text{ m}^3/\text{s}$]). Due to the Coriolis force, the sign of which switches across the equator, the EUC remains trapped along the equator as it travels eastward toward South America. Due a cross-equatorial (southerly) component of the prevailing trade winds in the eastern half of the basin, the dynamic boundary provided by the equator nudges the EUC to approximately $\frac{1}{4}^\circ$ south of the equator there [31–33]. The first topographic obstacle encountered by the EUC in the eastern Pacific is the westernmost (and youngest [34]) of the Galápagos Islands, Fernandina and Isabela. At the surface, Isabela stretches from 1.06°S to 0.17°N , and the bathymetric slopes from the western shores of these islands to the open-ocean seafloor are extremely steep. The Galápagos thus stands as a formidable barrier directly in the path of the EUC at 91.7°W . On geologic timescales (millions of years), changes in the distribution of islands have had detectable impacts on the regional ocean circulation and SST patterns [35]. It is therefore possible for subtle changes in the position or intensity of the EUC in the modern climate to have a large impact on upwelling and SST in the GCP—and profound consequences for the ecosystem.

Indeed, there have been impactful changes in the position and intensity of the EUC on its approach to the Galápagos in recent decades (Fig 4). Just upstream of the Galápagos (at 93°W), the EUC has been intensifying at a rate of 0.17 m/s (or by 29%) per 39 years. In addition to accelerating, the EUC has deepened by about 10 m (Fig 4B and 4C) and shifted slightly southward by about 10 km (Fig 4A and 4C). The acceleration and southward shift of the EUC

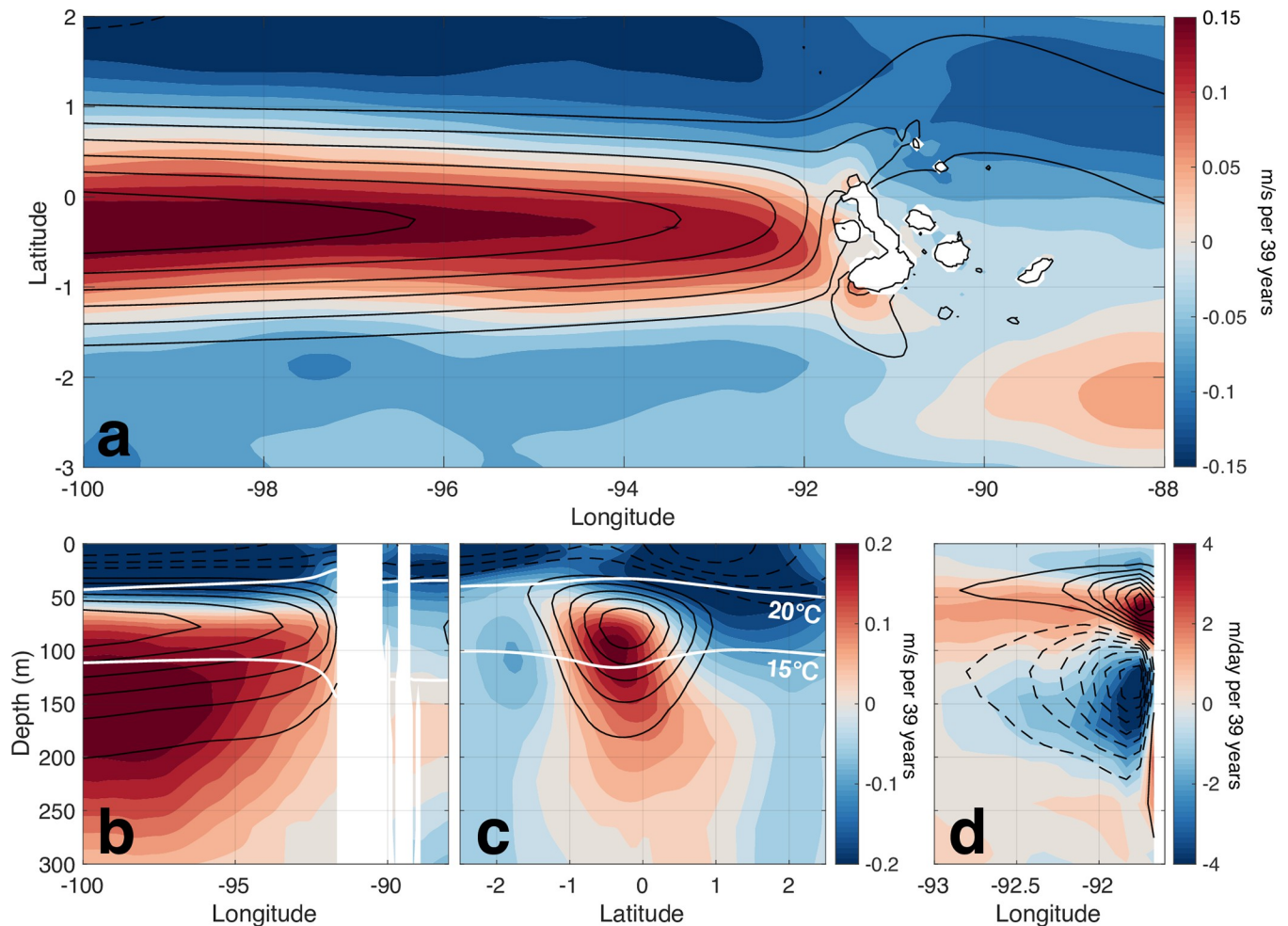


Fig 4. Estimated changes in equatorial ocean circulation. **a**, Trend in zonal ocean velocity (m/s per 39 years) averaged from 50–150 m depth. Black contours are the mean zonal velocity, contoured every 0.1 m/s; the outermost contour is 0.1 m/s. **b**, As in **a** but as an equatorial cross-section (averaged from 1°S–0.5°N). Dashed contours indicate negative or westward zonal velocity, the white contours denote the 15°C and 20°C isotherms, and white space represents the subsurface topography of the Galápagos Islands. **c**, As in **b** but as a north-south cross-section along 93°W. The color scale next to **c** applies to **b** and **c**. **d**, Equatorial cross-section (averaged from 0.9°S–0.2°N) of the trend in vertical ocean velocity (m/day per 39 years); black contours are the mean vertical velocity, contoured every 1 m/day.

<https://doi.org/10.1371/journal.pclm.0000056.g004>

are both conducive to stronger topographic upwelling. The increased zonal convergence as the faster EUC impinges upon the island must be balanced by increased divergence (a combination of meridional and vertical divergence), and the slightly more southward-biased EUC core brings it into better alignment with the islands, favoring upwelling over circumvention around the north of Isabela. Moreover, the deepening of the EUC core implies upwelling of deeper (and thus colder) water toward the surface. Analysis of trends in vertical velocity immediately west of the Galápagos confirms an intensification of vertical divergence about the depth at which the EUC meets the islands (Fig 4D), including a 54% increase in upwelling velocity above the EUC core (Fig 5C).

Not only has the eastward-flowing EUC accelerated, so too has the westward-flowing South Equatorial Current (SEC) near the surface (Fig 4B and 4C), resulting in a stronger vertical shear of horizontal velocity and greater potential for turbulent mixing. However, as ocean warming due to anthropogenic radiative forcing is surface intensified in general, the vertical density stratification may also increase, and these two competing influences on the vertical

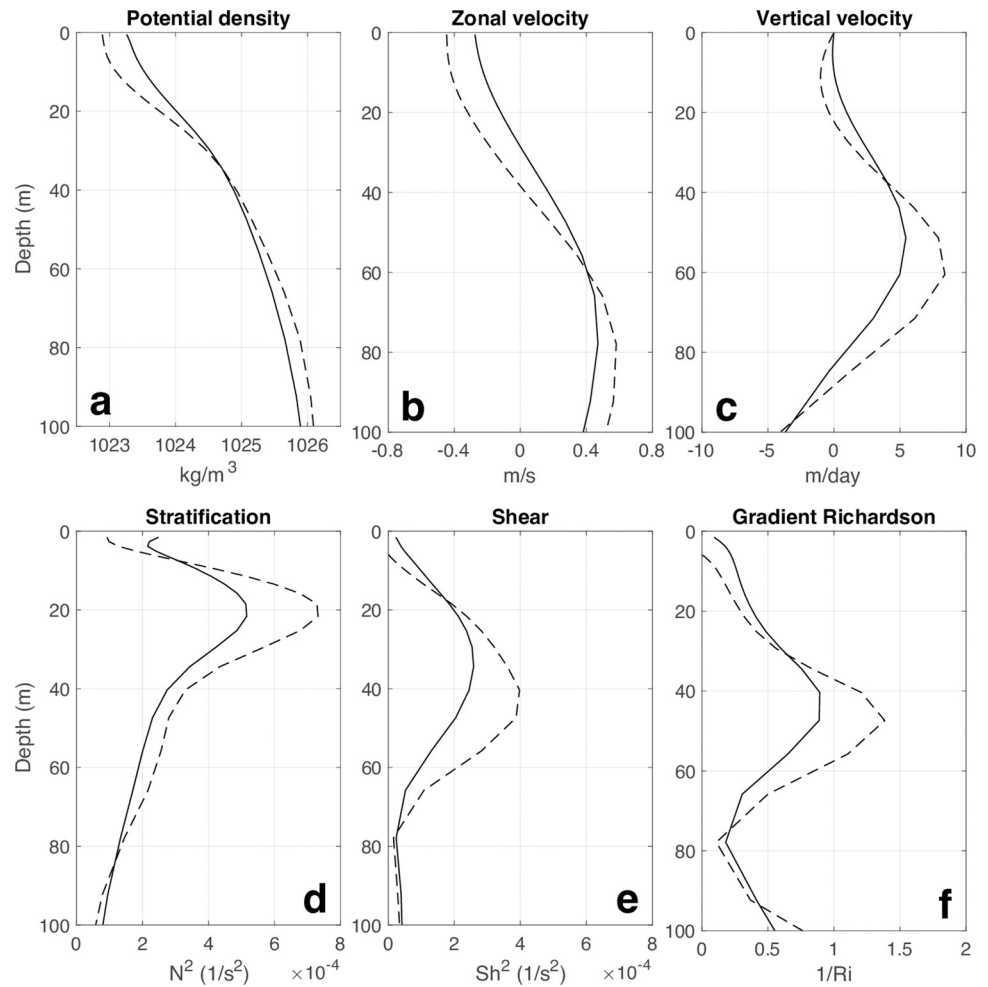


Fig 5. Changes in stratification and shear west of the Galápagos. **a**, Vertical profiles of potential density (kg/m^3) averaged throughout 1993–2018 (solid line) and with the addition of the trend in potential density per 39 years (dashed line). **b**, As in **a** but for zonal velocity (m/s). **c**, As in **a** but for vertical velocity (m/day). **d**, As in **a** but for buoyancy frequency squared (N^2 , $1/\text{s}^2$). **e**, As in **a** but for the vertical shear of zonal velocity squared (Sh^2 , $1/\text{s}^2$). **f**, As in **a** but for the inverse of the gradient Richardson number ($1/Ri$, dimensionless).

<https://doi.org/10.1371/journal.pclm.0000056.g005>

distribution of heat may introduce some complexity to the change in overall stability. Indeed, both stratification and shear increase near the thermocline and at the interface between the SEC and EUC (Fig 5). The resulting change in the gradient Richardson number, a scale with which we may weigh changes in stratification and shear relative to one another, indicates that the degree of vertical turbulent mixing and overturning has also increased beneath the GCP in recent decades (Fig 5F).

A southerly kick in the atmosphere

The combination of a faster, deeper and better-aligned EUC that is driving an acceleration of topographic upwelling, and a sheared environment that is more conducive to turbulent mixing, is consistent with the robust cooling trend observed west of the Galápagos since 1982. Why, then, has the EUC been changing in this way? As an integral part of the wind-driven equatorial ocean circulation, it is natural to consider the concurrent changes in the surface wind field. Over the recent decades, an anomalous southward sea level pressure gradient has

emerged (Fig 6A), which drives a southerly acceleration by about 1 m/s. South of the equator, the implied anomalous zonal Ekman transports (westward, $U_E < 0$) and their configuration relative to the mean sea surface height gradients ($h_x < 0$) implies an overall negative zonal advection of thickness ($-U_E h_x < 0$), contributing to the observed relative minimum in the sea surface height trend extending westward from the Galápagos and centered just south of the equator (Fig 6B). North of the equator (along $\sim 2^\circ\text{N}$), the surface wind trend is quite parallel to the mean sea surface height gradient, therefore no such advective response emerges there. Evidently, the Galápagos Islands influence not only the mean sea surface height field (with a local minimum directly adjacent to the islands), but also the surface wind trends (Fig 6B). While the broader, southerly wind trend corresponds to horizontal gradients in the SST and SLP trends [36], a local reduction of wind speed also occurs directly over the GCP where SST has been cooling, consistent with the implied increase in atmospheric boundary layer stability and reduced momentum mixing with the free troposphere [37, 38].

From the meridional gradients in the resulting sea surface height trend (h_y), it is straightforward to predict the trends in zonal velocity by geostrophic balance ($fu_g = -gh_y$, where f is the Coriolis parameter). Such predictions are qualitatively reasonable for the surface currents (Fig 7), especially given neglect of the Ekman component in these calculations, which would reduce (increase) the westward trends north (south) of the equator, bringing the predictions into better agreement with the actual surface current trends. This confirms that the acceleration of the SEC is largely explained by the pattern of sea level change, which is explained by the alignment of the surface wind trend relative to the gradients in the mean sea surface height field. The acceleration of the EUC is then simply a consequence of the requirement for zonal mass transports to balance (*i.e.*, more water is piled to the west, which increases the eastward pressure gradient force driving the EUC), the deepening of the EUC is a consequence of greater momentum mixing, and the southward shift of the EUC core is a direct consequence of the southerly wind trend (as in the reason the EUC is shifted slightly southward of the equator to begin with). Any one of these changes in the equatorial ocean circulation would, in isolation, represent a conceivable explanation for the observed cooling trend in the GCP. Together, they provide an unambiguous attribution of the cooling trend as a fingerprint of a wholesale change in the wind-driven equatorial ocean circulation.

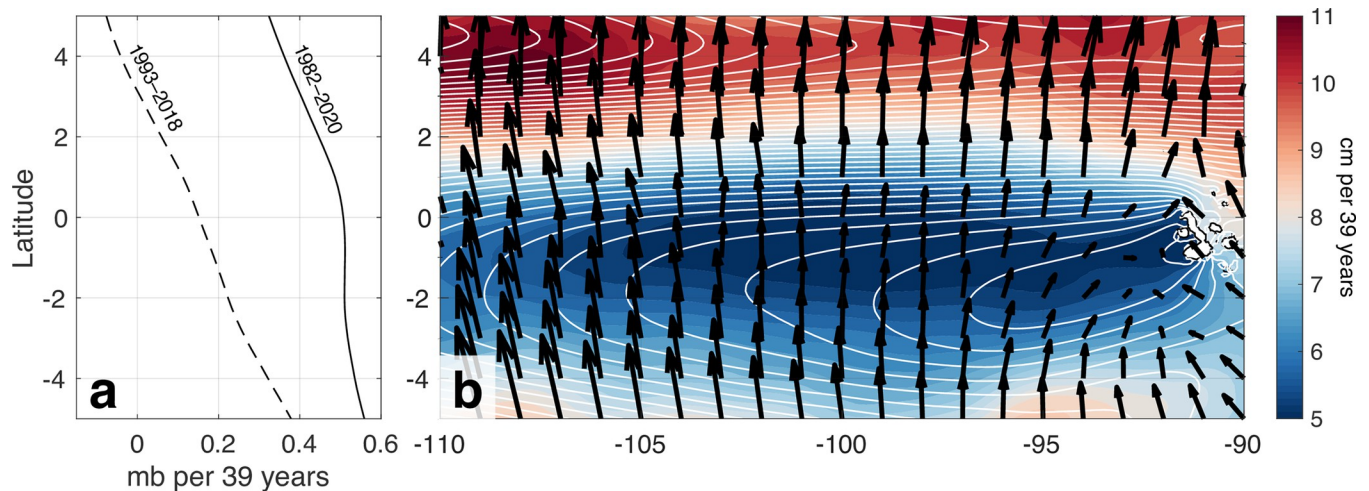


Fig 6. Changes in surface wind and sea level. **a**, Latitudinal profiles of observed sea level pressure trends (mb per 39 years) averaged from 110°W to 100°W computed over the periods 1982–2020 (solid line) and 1993–2018 (dashed line). **b**, Trends in 10-m wind velocity (vectors) and sea surface height (cm per 39 years, colors). White contours in **b** are the mean sea surface height, contoured every 0.5 cm; to the southwest of the Galápagos is a region of relatively low mean sea surface height. The magnitude of the southerly 10-m wind trends is ~ 1 m/s per 39 years.

<https://doi.org/10.1371/journal.pclm.0000056.g006>

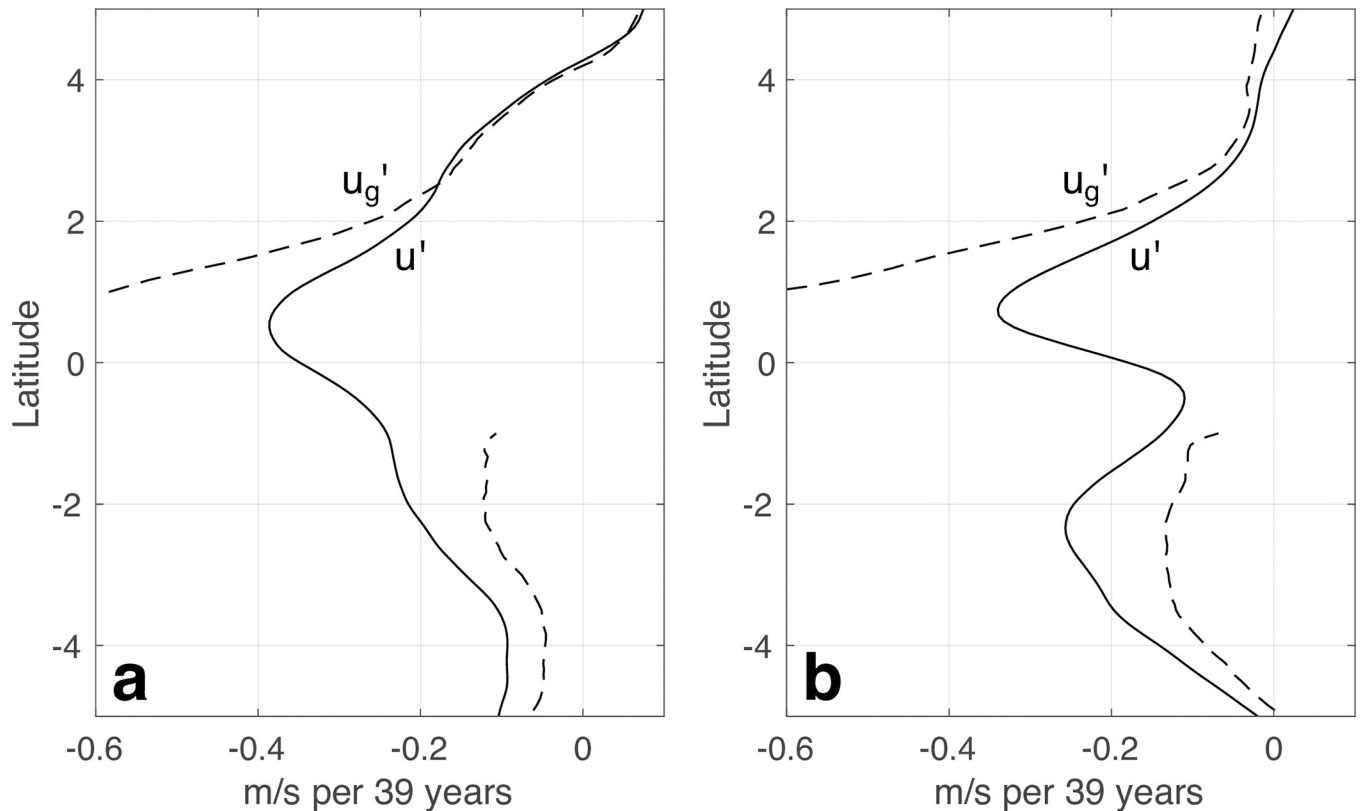


Fig 7. Changes in surface currents and geostrophy. **a**, Latitudinal profile of the trend in surface zonal velocity (m/s per 39 years, solid line) at 100°W, and that predicted by geostrophic balance (dashed line), which is proportional to the latitudinal slope of the sea surface height trend. **b**, As in **a** but at 93°W. Zonal geostrophic velocity is not shown within $\pm 1^\circ$ latitude since $f=0$ at the equator, but approximation of the zonal geostrophic velocity on the equator by the method of equatorial geostrophy [39] confirms that the predicted surface current trend is negative (*i.e.*, westward) there (not shown).

<https://doi.org/10.1371/journal.pclm.0000056.g007>

Discussion and conclusions

A cooling trend in the GCP is robust over a period of almost four decades of satellite observations (1982–2020), and indicators and diagnostics of changes in equatorial oceanography from a high-resolution ocean state estimate spanning two thirds of that time period (1993–2018) shed light on a physical mechanism. The mechanism begins with an acceleration of the cross-equatorial component of the trade winds in the eastern Pacific, driven by an interhemispheric gradient in surface warming, which is an emergent feature of the pattern of warming (past and future) in response to anthropogenic radiative forcing [40, 41]. Interestingly, the southerly wind trend is also consistent with the observed cooling trend in the GCP from the perspective of a newly proposed mechanism for upwelling that links local southerly winds with vigorous local submesoscale circulations [16].

Regardless, this is not a direct attribution to anthropogenic forcing. The long-term evolution of the meridional surface winds in the region is also necessarily linked to concurrent changes in the intertropical convergence zone (ITCZ), which has a complex and uncertain response to radiative forcing [42] and is subject to considerable internal climate variability. Whether and the extent to which the changes diagnosed for recent decades can sustain the cooling trend in the GCP in the decades to come, outpacing surface radiative forcing and an increasing tendency for vertical stratification, is uncertain and may require very high-resolution global climate models (GCMs) that are similarly able to capture the complex Galápagos

bathymetry and the delicate dynamical balances governing the coupled atmosphere and ocean in the eastern equatorial Pacific. While several studies have indicated that the EUC is projected to accelerate under future climate forcing scenarios in coupled GCMs [22, 23, 43, 44], *ensembles* of very high-resolution GCMs may be needed to further disambiguate the role of internal variability in the observed SST trends and changes in circulation. Unfortunately, we may be some ways from ensembles of GCMs capable of adequately resolving the Galápagos, or the detailed dynamics of the EUC for that matter.

Interestingly, the results of this study have brought forth a mechanism that could also explain the apparent refusal thus far of the broader eastern equatorial Pacific Ocean (not just the GCP) to warm—or to warm by as much as the rest of the tropics including the western equatorial Pacific, since the late 19th century [45–47]. The increased topographic upwelling implied by the changes in the strength and position of the EUC in the eastern Pacific uniquely impact the GCP, but the increase in vertical shear of zonal velocity along the equator extends well into the central Pacific (Fig 8). It is therefore possible that increased shear-induced mixing has played a role in maintaining (or even strengthening) the zonal SST gradient along the equatorial Pacific, along with other mechanisms proposed earlier [48–52], and the GCP is merely an early sentinel of that signal by virtue of its extremely shallow thermocline. Several other physical mechanisms may be important in the open equatorial ocean, west of the GCP. For example, zonal advection appears to play a mechanistic role in the changing circulation within the broader domain (*e.g.*, Fig 6B), but a calculation of the zonal temperature advection term in the mixed layer heat budget *within* the GCP reveals negligible contribution to its cooling trend, clearly owing to the islands deflecting the SEC around the GCP (not shown).

Thus far, and for perhaps the very near future, the western shores of the Galápagos appear to be a safe haven from some of the deleterious impacts of anthropogenic climate change including ocean warming and suppression of upwelling. El Niño events will continue to happen every few years, accompanied by a temporary reduction of EUC velocity [28, 30, 53] and upwelling, extreme SST warming, and a general ravaging of the entire ecosystem from

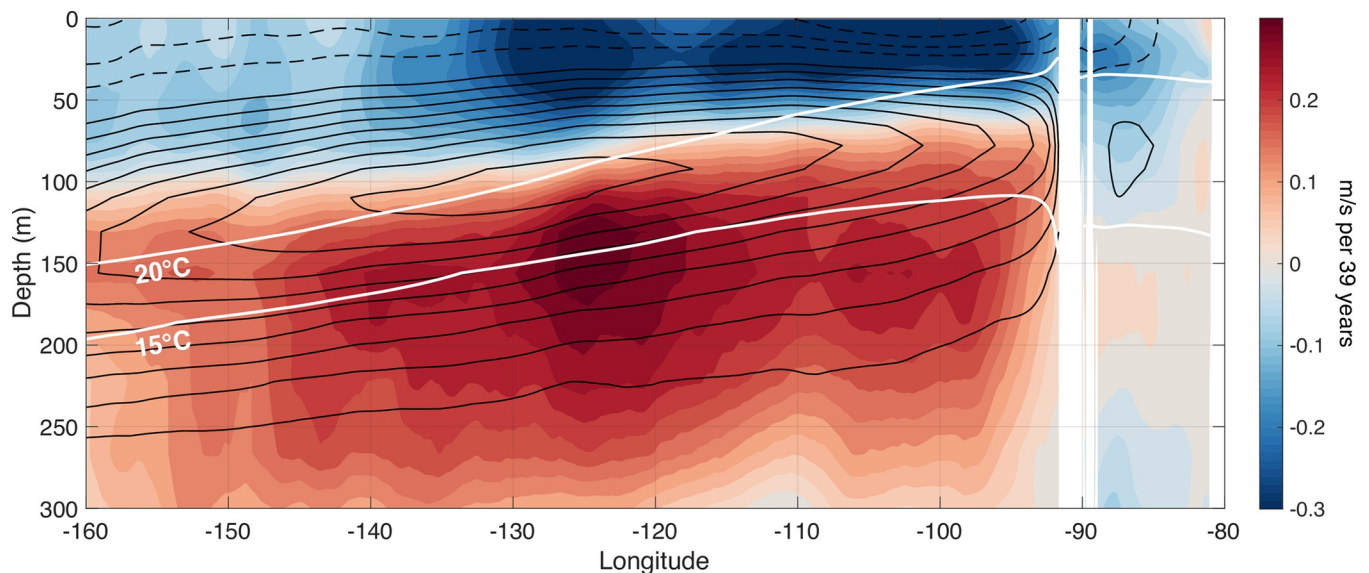


Fig 8. Estimated changes in equatorial ocean circulation. Trend in zonal ocean velocity (m/s per 39 years) as an equatorial cross-section (averaged from 1°S–0.5°N). Black contours are the mean zonal velocity, contoured every 0.1 m/s; the outermost contour is 0.1 m/s. Dashed contours indicate negative or westward zonal velocity, the white contours denote the 15°C and 20°C isotherms, and white space near 90°W represents the subsurface topography of the Galápagos Islands. This is as in Fig 4B but extending further westward.

<https://doi.org/10.1371/journal.pclm.0000056.g008>

plankton to penguins [54, 55]. This region and its potential status as a safe haven is also quite distinct from other waters within the archipelago, where a cooling trend is not observed and heat-induced coral bleaching is periodically documented [56]. Challenges to the sustainable management and protection of the second largest marine reserve in the world notwithstanding, the recent trends detected and diagnosed here are cause for cautious optimism for some of the Ecuadorian fisheries, and the penguin population—virtually all of which are already clever enough to live along the western shores of Isabela and Fernandina.

Acknowledgments

The author acknowledges support from the NASA Sea Level Change Science Program, Award 80NSSC20K1123. The author also thanks the Mercator Ocean Service Desk (Véronique Landes) and Dr. Aneesh Subramanian for assistance with acquiring GLORYS-12v1 vertical ocean velocity fields.

Author Contributions

Conceptualization: Kristopher B. Karnauskas.

Formal analysis: Kristopher B. Karnauskas.

Funding acquisition: Kristopher B. Karnauskas.

Investigation: Kristopher B. Karnauskas.

Methodology: Kristopher B. Karnauskas.

Visualization: Kristopher B. Karnauskas.

Writing – original draft: Kristopher B. Karnauskas.

Writing – review & editing: Kristopher B. Karnauskas.

References

1. Caesar L, Rahmstorf S, Robinson A, Feulner G, Saba V. Observed fingerprint of a weakening Atlantic Ocean overturning circulation. *Nature*. 2018 Apr; 556(7700):191–6. <https://doi.org/10.1038/s41586-018-0006-5> PMID: 29643485
2. Liu W, Fedorov AV, Xie SP, Hu S. Climate impacts of a weakened Atlantic Meridional Overturning Circulation in a warming climate. *Sci Adv*. 2020 Jun; 6(26):eaaz4876. <https://doi.org/10.1126/sciadv.aaz4876> PMID: 32637596
3. Karnauskas KB, Jenouvrier S, Brown CW, Murtugudde R. Strong sea surface cooling in the eastern equatorial Pacific and implications for Galápagos Penguin conservation: OCEAN COOLING AND GALÁPAGOS PENGUINS. *Geophys Res Lett*. 2015 Aug 16; 42(15):6432–7.
4. Paltán HA, Benitez FL, Rosero P, Escobar-Camacho D, Cuesta F, Mena CF. Climate and sea surface trends in the Galapagos Islands. *Sci Rep*. 2021 Dec; 11(1):14465. <https://doi.org/10.1038/s41598-021-93870-w> PMID: 34262105
5. IUCN. *Spheniscus mendiculus*: BirdLife International: The IUCN Red List of Threatened Species 2020: e.T22697825A182729677 [Internet]. International Union for Conservation of Nature; 2020 [cited 2021 Mar 11]. Available from: <https://www.iucnredlist.org/species/22697825/182729677>
6. IUCN. *Arctocephalus galapagoensis*: Trillmich, F.: The IUCN Red List of Threatened Species 2015: e.T2057A45223722 [Internet]. International Union for Conservation of Nature; 2014 [cited 2021 Mar 11]. Available from: <http://www.iucnredlist.org/details/2057/0>
7. IUCN. *Zalophus wollebaeki*: Trillmich, F.: The IUCN Red List of Threatened Species 2015: e.T41668A45230540 [Internet]. International Union for Conservation of Nature; 2014 [cited 2021 Mar 11]. Available from: <http://www.iucnredlist.org/details/41668/0>
8. UNESCO World Heritage Convention. Galápagos Islands [Internet]. UNESCO World Heritage Convention; [cited 2021 Mar 11]. Available from: <https://whc.unesco.org/en/list/1/>

9. Rasmusson EM, Wallace JM. Meteorological Aspects of the El Niño/Southern Oscillation. *Science*. 1983 Dec 16; 222(4629):1195–202. <https://doi.org/10.1126/science.222.4629.1195> PMID: 17806710
10. Chatterjee A, Gierach MM, Sutton AJ, Feely RA, Crisp D, Eldering A, et al. Influence of El Niño on atmospheric CO₂ over the tropical Pacific Ocean: Findings from NASA's OCO-2 mission. *Science*. 2017 Oct 13; 358(6360):eaam5776. <https://doi.org/10.1126/science.aam5776> PMID: 29026014
11. Eden C. The influence of the Galápagos Islands on tropical temperatures, currents and the generation of tropical instability waves. *Geophys Res Lett*. 2004; 31(15):L15308.
12. Karnauskas KB, Murtugudde R, Busalacchi AJ. The Effect of the Galápagos Islands on the Equatorial Pacific Cold Tongue. *Journal of Physical Oceanography*. 2007 May 1; 37(5):1266–81.
13. Karnauskas KB, Murtugudde R, Busalacchi AJ. The Effect of the Galápagos Islands on ENSO in Forced Ocean and Hybrid Coupled Models. *Journal of Physical Oceanography*. 2008 Nov 1; 38(11):2519–34.
14. Karnauskas KB, Murtugudde R, Owens WB. Climate and the Global Reach of the Galápagos Archipelago: State of the Knowledge. In: Harpp KS, Mittelstaedt E, d'Ozouville N, Graham DW, editors. *Geophysical Monograph Series* [Internet]. Hoboken, New Jersey: John Wiley & Sons, Inc; 2014 [cited 2021 Mar 11]. p. 215–31. Available from: <http://doi.wiley.com/10.1002/9781118852538.ch11>
15. Houvenaghel GT. Oceanographic Conditions in the Galapagos Archipelago and Their Relationships with Life on the Islands. In: Boje R, Tomczak M, editors. *Upwelling Ecosystems* [Internet]. Berlin, Heidelberg: Springer Berlin Heidelberg; 1978 [cited 2021 Mar 11]. p. 181–200. Available from: http://link.springer.com/10.1007/978-3-642-66985-9_15
16. Forryan A, Naveira Garabato AC, Vic C, Nurser AJG, Hearn AR. Galápagos upwelling driven by localized wind–front interactions. *Sci Rep*. 2021 Dec; 11(1):1277. <https://doi.org/10.1038/s41598-020-80609-2> PMID: 33446722
17. Boersma PD, Steinfurth A, Merlen G, Jiménez–Uzcátegui G, Vargas F, Parker PG. Galápagos Penguin (*Spheniscus mendiculus*). In: *Penguins Natural History and Conservation*. University of Washington Press; 2013. p. 360.
18. Trillmich F. Galápagos Fur Seal (*Arctocephalus galapagoensis*, Heller 1904). In: *ECOLOGY AND CONSERVATION OF PINNIPEDS IN LATIN AMERICA* [Internet]. S.l.: SPRINGER; 2021 [cited 2021 Mar 11]. p. 31–50. Available from: <http://public.eblib.com/choice/PublicFullRecord.aspx?p=6501094>
19. Krüger O. Galápagos Sea Lion (*Zalophus wollebaeki*, Sivertsen 1953). In: *ECOLOGY AND CONSERVATION OF PINNIPEDS IN LATIN AMERICA* [Internet]. S.l.: SPRINGER; 2021 [cited 2021 Mar 11]. p. 145–63. Available from: <http://public.eblib.com/choice/PublicFullRecord.aspx?p=6501094>
20. Reynolds RW, Rayner NA, Smith TM, Stokes DC, Wang W. An Improved In Situ and Satellite SST Analysis for Climate. *Journal of Climate*. 2002 Jul 1; 15(13):1609–25.
21. Vargas H, Loughheed C, Snell H. Population size and trends of the Galápagos Penguin *Spheniscus mendiculus*: Population size and trends of the Galápagos Penguin. *Ibis*. 2005 Mar 7; 147(2):367–74.
22. Karnauskas KB, Cohen AL. Equatorial refuge amid tropical warming. *Nature Clim Change*. 2012 Jul; 2(7):530–4.
23. Karnauskas KB, Cohen AL, Gove JM. Mitigation of Coral Reef Warming Across the Central Pacific by the Equatorial Undercurrent: A Past and Future Divide. *Sci Rep*. 2016 Aug; 6(1):21213. <https://doi.org/10.1038/srep21213> PMID: 26880042
24. Lellouche JM, Greiner E, Le Galloudec O, Garric G, Regnier C, Drevillon M, et al. Recent updates to the Copernicus Marine Service global ocean monitoring and forecasting real-time 1/12° high-resolution system. *Ocean Sci*. 2018 Sep 25; 14(5):1093–126.
25. Hersbach H, Bell B, Berrisford P, Hirahara S, Horányi A, Muñoz-Sabater J, et al. The ERA5 global reanalysis. *QJR Meteorol Soc*. 2020 Jul; 146(730):1999–2049.
26. Worley SJ, Woodruff SD, Reynolds RW, Lubker SJ, Lott N. ICOADS release 2.1 data and products. *Int J Climatol*. 2005 Jun 15; 25(7):823–42.
27. Karnauskas KB, Jakoboski J, Johnston TMS, Owens WB, Rudnick DL, Todd RE. The Pacific Equatorial Undercurrent in Three Generations of Global Climate Models and Glider Observations. *J Geophys Res Oceans* [Internet]. 2020 Nov [cited 2021 Mar 11]; 125(11). Available from: <https://onlinelibrary.wiley.com/doi/10.1029/2020JC016609>
28. Rudnick DL, Owens WB, Johnston TMS, Karnauskas KB, Jakoboski J, Todd RE. The Equatorial Current System West of the Galápagos Islands during the 2014–16 El Niño as Observed by Underwater Gliders. *Journal of Physical Oceanography*. 2021 Jan; 51(1):3–17.
29. Kanamitsu M, Ebisuzaki W, Woollen J, Yang SK, Hnilo JJ, Fiorino M, et al. NCEP–DOE AMIP-II Reanalysis (R-2). *Bull Amer Meteor Soc*. 2002 Nov; 83(11):1631–44.

30. Johnson GC, Sloyan BM, Kessler WS, McTaggart KE. Direct measurements of upper ocean currents and water properties across the tropical Pacific during the 1990s. *Progress in Oceanography*. 2002 Jan; 52(1):31–61.
31. Charney JG, Spiegel SL. Structure of Wind-Driven Equatorial Currents in Homogeneous Oceans. *Journal of Physical Oceanography*. 1971 Jul 1; 1(3):149–60.
32. Philander SGH, Delecluse P. Coastal currents in low latitudes (with application to the Somali and El Niño currents). *Deep Sea Research Part A Oceanographic Research Papers*. 1983 Aug; 30(8):887–902.
33. Kessler WS, Rothstein LM, Chen D. The Annual Cycle of SST in the Eastern Tropical Pacific, Diagnosed in an Ocean GCM. *Journal of Climate*. 1998 May 1; 11(5):777–99.
34. Geist DJ, Snell H, Snell H, Goddard C, Kurz MD. A Paleogeographic Model of the Galápagos Islands and Biogeographical and Evolutionary Implications. In: Harpp KS, Mittelstaedt E, d'Ozouville N, Graham DW, editors. *Geophysical Monograph Series* [Internet]. Hoboken, New Jersey: John Wiley & Sons, Inc; 2014 [cited 2021 Mar 11]. p. 145–66. Available from: <http://doi.wiley.com/10.1002/9781118852538.ch8>
35. Karnauskas KB, Mittelstaedt E, Murtugudde R. Paleooceanography of the eastern equatorial Pacific over the past 4 million years and the geologic origins of modern Galápagos upwelling. *Earth and Planetary Science Letters*. 2017 Feb; 460:22–8.
36. Lindzen RS, Nigam S. On the Role of Sea Surface Temperature Gradients in Forcing Low-Level Winds and Convergence in the Tropics. *Journal of Atmospheric Sciences*. 1987 Sep 1; 44(17):2418–36.
37. Hayes SP, McPhaden MJ, Wallace JM. The Influence of Sea-Surface Temperature on Surface Wind in the Eastern Equatorial Pacific: Weekly to Monthly Variability. *Journal of Climate*. 1989 Dec 1; 2(12):1500–6.
38. Wallace JM, Mitchell TP, Deser C. The Influence of Sea-Surface Temperature on Surface Wind in the Eastern Equatorial Pacific: Seasonal and Interannual Variability. *Journal of Climate*. 1989 Dec 1; 2(12):1492–9.
39. Meinen CS, McPhaden MJ, Johnson GC. Vertical Velocities and Transports in the Equatorial Pacific during 1993–99*. *J Phys Oceanogr*. 2001 Nov; 31(11):3230–48.
40. Intergovernmental Panel on Climate Change, editor. Detection and Attribution of Climate Change: from Global to Regional. In: *Climate Change 2013—The Physical Science Basis* [Internet]. Cambridge: Cambridge University Press; 2014 [cited 2021 Mar 11]. p. 867–952. Available from: https://www.cambridge.org/core/product/identifier/CBO9781107415324A030/type/book_part
41. Intergovernmental Panel on Climate Change, editor. Long-term Climate Change: Projections, Commitments and Irreversibility Pages 1029 to 1076. In: *Climate Change 2013—The Physical Science Basis* [Internet]. Cambridge: Cambridge University Press; 2014 [cited 2021 Mar 11]. p. 1029–136. Available from: https://www.cambridge.org/core/product/identifier/CBO9781107415324A032/type/book_part
42. Byrne MP, Pendergrass AG, Rapp AD, Wodzicki KR. Response of the Intertropical Convergence Zone to Climate Change: Location, Width, and Strength. *Curr Clim Change Rep*. 2018 Dec; 4(4):355–70. <https://doi.org/10.1007/s40641-018-0110-5> PMID: 30931244
43. Luo Y, Rothstein LM, Zhang RH. Response of Pacific subtropical-tropical thermocline water pathways and transports to global warming. *Geophys Res Lett*. 2009 Feb 17; 36(4):L04601.
44. Sen Gupta A, Ganachaud A, McGregor S, Brown JN, Muir L. Drivers of the projected changes to the Pacific Ocean equatorial circulation: PACIFIC OCEAN CIRCULATION PROJECTIONS. *Geophys Res Lett*. 2012 May; 39(9):n/a–n/a.
45. Karnauskas KB, Seager R, Kaplan A, Kushnir Y, Cane MA. Observed Strengthening of the Zonal Sea Surface Temperature Gradient across the Equatorial Pacific Ocean*. *Journal of Climate*. 2009 Aug 15; 22(16):4316–21.
46. Solomon A, Newman M. Reconciling disparate twentieth-century Indo-Pacific ocean temperature trends in the instrumental record. *Nature Clim Change*. 2012 Sep; 2(9):691–9.
47. Seager R, Cane M, Henderson N, Lee DE, Abernathey R, Zhang H. Strengthening tropical Pacific zonal sea surface temperature gradient consistent with rising greenhouse gases. *Nat Clim Chang*. 2019 Jul; 9(7):517–22.
48. Clement AC, Seager R, Cane MA, Zebiak SE. An Ocean Dynamical Thermostat. *Journal of Climate*. 1996 Sep 1; 9(9):2190–6.
49. Seager R, Murtugudde R. Ocean Dynamics, Thermocline Adjustment, and Regulation of Tropical SST. *Journal of Climate*. 1997 Mar 1; 10(3):521–34.
50. Sun DZ, Liu Z. Dynamic Ocean-Atmosphere Coupling: A Thermostat for the Tropics. *Science*. 1996 May 24; 272(5265):1148–50. <https://doi.org/10.1126/science.272.5265.1148> PMID: 8662447

51. Zhang L, Li T. A Simple Analytical Model for Understanding the Formation of Sea Surface Temperature Patterns under Global Warming*. *Journal of Climate*. 2014 Nov 15; 27(22):8413–21.
52. Coats S, Karnauskas KB. A Role for the Equatorial Undercurrent in the Ocean Dynamical Thermostat. *J Climate*. 2018 Aug; 31(16):6245–61.
53. Firing E, Lukas R, Sadler J, Wyrski K. Equatorial Undercurrent Disappears During 1982–1983 El Niño. *Science*. 1983 Dec 9; 222(4628):1121–3. <https://doi.org/10.1126/science.222.4628.1121> PMID: 17747385
54. Feldman G, Clark D, Halpern D. Satellite Color Observations of the Phytoplankton Distribution in the Eastern Equatorial Pacific During the 1982–1983. El Niño. *Science*. 1984 Nov 30; 226(4678):1069–71.
55. Boersma PD. Population Trends of the Galápagos Penguin: Impacts of El Niño and La Niña. *The Condor*. 1998 May; 100(2):245–53.
56. Cavole LM, DeCarlo TM. Early observations of heat-induced coral bleaching in the Galápagos Islands. *Reef Encounters*. 2020 Jul; 35(1):68–72.